Available online at www.sciencedirect.com

ScienceDirect

Progress in Natural Science: Materials International 24 (2014) 199–204

Progress in Natural Science Materials International

www.elsevier.com/locate/pnsmi
www.sciencedirect.com

Original Research

Competing crystallite size and zinc concentration in silica coated cobalt ferrite nanoparticles

K. Nadeem*, M. Shahid, M. Mumtaz

Materials Research Laboratory, Department of Physics, International Islamic University, Islamabad, Pakistan

Received 10 October 2013; accepted 12 May 2014
Available online 3 June 2014

Abstract

Silica coated (30 wt%) cobalt zinc ferrite ($Co_{1-x}Zn_xFe_2O_4$, $x=0$, 0.2, 0.3, 0.4, 0.5 and 1) nanoparticles were synthesized by using sol–gel method. Silica acts as a spacer among the nanoparticles to avoid the agglomeration. X-ray diffraction (XRD) reveals the cubic spinel ferrite structure of nanoparticles with crystallite size in the range 37–45 nm. Fourier transform infrared (FTIR) spectroscopy confirmed the formation of spinel ferrite and SiO_2. Scanning electron microscopy (SEM) images show that the nanoparticles are nearly spherical and non-agglomerated due to presence of non-magnetic SiO_2 surface coating. All these measurements signify that the structural and magnetic properties of $Co_{1-x}Zn_xFe_2O_4$ ferrite nanoparticles strongly depend on Zn concentration and nanoparticle average crystallite size in different Zn concentration regimes.

Keywords: Ferrite; Nanoparticles; Composites; Magnetic properties

1. Introduction

Magnetic nanoparticles are of great importance due to their potential applications in ferro-fluids, targeted drug delivery, magnetic data storage, and cancer treatment [1–3]. The magnetization of fine nanoparticles is significantly different as compared to that of their counter bulk material [4]. Ferro- or ferri-magnetic nanoparticles have lower saturation magnetization as compared to their counter bulk material [5]. This reduction of magnetization is a well known effect and attributed to the presence of disordered surface spins on individual nanoparticle's surface. Due to broken surface bonds and different surface anisotropy, surface spins have different magnetic orientations as compared to spins in the core of the nanoparticles [6,7]. In ferrite nanoparticle, the surface effects are induced due to disordered surface spins which can affect their magnetic properties [8,9]. These surface effects get more pronounced with decreasing particle size due to large surface to volume ratio. Magnetic properties of the bulk spinel ferrite materials also depend upon the cationic distribution on the octahedral [A] and tetrahedral [B] lattice sites [10]. The spins at the octahedral and tetrahedral lattice sites are opposite to each other. Therefore it is important to take into account the nanoparticle crystallite size during the investigation of doping effects in ferrite nanoparticles. Different researchers have made several attempts for the improvement of the magnetic properties of cobalt ferrite ($CoFe_2O_4$) nanoparticles by doping with different cations [11–14]. It is reported that the nature of the dopant (e.g. ionic radii, mobility, polarization, anisotropy, etc.) also affects the properties of the ferrites [15,16]. Zn^{2+} ions are non-magnetic but they can increase the net magnetization of $CoFe_2O_4$ [17,18]. This increase in magnetization is due to rearrangement of cations on the lattice sites. Actually the local magnetizations at the two lattice sites (octahedral [A] and tetrahedral [B]) in cobalt ferrite are opposite in direction, which get disturbed upon doping of Zn^{2+} cations [19]. Different reports confirmed the rearrangement of the cations

*Corresponding author. Tel.: +92 51 9019714.
E-mail address: kashif.nadeem@iiu.edu.pk (K. Nadeem).
Peer review under responsibility of Chinese Materials Research Society.

Production and hosting by Elsevier

http://dx.doi.org/10.1016/j.pnsc.2014.05.011

on the lattice sites in $CoFe_2O_4$ upon doping by using Mössbauer spectroscopy [20–22]. Therefore, one can increase the net magnetization of the $CoFe_2O_4$ nanoparticles by doping it with particular concentration of the Zn^{2+} cations. However, this particular concentration for the maximum (peak) magnetization is reported by several scientists with different results e.g., Hou et al. [23] reported the peak magnetization (64.6 emu/g) at $x=0.5$ Zn concentration in $CoFe_2O_4$ nanospheres synthesized by using a solvothermal method; Singhal et al. [17] reported the peak magnetization (91.6 emu/g) at $x=0.4$ Zn concentration in $CoFe_2O_4$ nanoparticles prepared by using sol–gel method; Somaiah et al. [24] reported the peak magnetization (87 emu/g) at $x=0.2$ Zn concentration in nano $CoFe_2O_4$ synthesized by using an auto-combustion technique; Rani et al. [25] reported the peak magnetization at $x=0.1$ Zn concentration in nano $CoFe_2O_4$ prepared by using a solution combustion method. The contradiction in the optimum Zn concentration for the peak magnetization can be due to different reasons, e.g. different synthesis methods, different synthesis conditions, annealing temperatures and different crystallite sizes.

Magnetic nanoparticles have strong tendency to aggregate due to magnetic interparticle interactions and large nanoparticle surface reactivity, which can give a collective or different magnetic response as compared to non-agglomerated nanoparticles. To avoid agglomeration, different routes had been adopted, e.g. disperse nanoparticles in non-magnetic matrix, surface silica coating, polymer coating etc. [26–29]. In this study, we have used silica (SiO_2) as a nanoparticle's surface coating material, which also acts as a spacer among the nanoparticles and reduces agglomeration/inter-particles interactions. In this article, we have studied the structural and magnetic properties of the SiO_2 coated zinc doped cobalt ferrite ($Co_{1-x}Zn_xFe_2O_4$, Zn concentration (x)=0, 0.2, 0.3, 0.4, 0.5 and 1) nanoparticles synthesized by using the sol–gel method. We tried our best to keep the experimental conditions constant but still we got some scatter in the average crystallite size with Zn concentration (x). We have considered the variation in the nanoparticle crystallite size with x during investigation of doping effects.

2. Synthesis and experimental techniques

Synthesis schemes play an important role in controlling the properties of SiO_2 coated magnetic nanoparticles [30]. Sol–gel, co-precipitation, condensation procedure, microemulsion route, etc. are commonly used methods to coat nanoparticles with SiO_2 for their surface modification [31,32]. Among them, the sol–gel method is a simple chemical method, which has been extensively used for the coating of nanoparticles with SiO_2 layer [27,33,34]. Therefore, we used the sol–gel method for the synthesis of SiO_2 coated $Co_{1-x}Zn_xFe_2O_4$ (where x=0, 0.2, 0.3, 0.4, 0.5 and 1) nanoparticles. The chemical reagents used were cobalt nitrate ($Co(NO_3)_2\cdot 6H_2O$), zinc nitrate ($Zn(NO_3)_2\cdot 6H_2O$), iron nitrate ($Fe(NO_3)_3\cdot 9H_2O$), citric acid ($C_6H_8O_7$), and tetraethyl orthosilicate ($Si(OC_2H_5)_4$) (TEOS, a precursor for SiO_2). The chemicals were purchased from Sigma-Aldrich. All the chemical reagents were of analytical grade and used without any purification.

First of all, a solution of $Co(NO_3)_2\cdot 6H_2O$, $Zn(NO_3)_2\cdot 6H_2O$, and $Fe(NO_3)_3\cdot 9H_2O$ in their stoichiometry was prepared in ethanol and was named as solution 1. Magnetic stirring was done to get a homogeneous mixture. Another solution 2 of the calculated amount of $C_6H_8O_7$ (molar ratio nitrates to citric acid=1:1) in distilled water was prepared and dropped into solution 1 under stirring to get a homogeneous combined solution. Afterwards TEOS (30 wt% of total nitrates) was dropped into the above combined solution under stirring. We kept the concentration of TEOS constant for the all the samples because SiO_2 concentration can affect the nanoparticle crystallite size. Now ammonia was added to get the pH value of about 5. The final solution was heated to 70 °C and stirred until the formation of wet gel. The wet gel was then placed in an oven at 100 °C overnight to remove the remaining water and ethanol. The dried gel was then ground in agate and mortar and annealed in a furnace at 900 °C for 2 h to get the desired SiO_2 coated cobalt zinc ferrite nanoparticles. The structural analysis was done by using X-ray diffraction (XRD) (D/Max IIIC Rigaku with a CuKα source of wavelength 1.54056 Å). The phonon modes were observed by using a Fourier transform infrared (FTIR) (Nicolet 5700) spectrometer in the wave number range 400–1200 cm^{-1}. Nanoparticles' imaging was done by using scanning electron microscopy (JEOL-instrument JSM-6490A). Magnetic measurements were taken by using a vibrating sample magnetometer (VSM).

3. Results and discussion

X-ray diffraction (XRD) was carried out using CuKα (0.154 nm) source at ambient pressure and temperature to study the structural parameters such as phase formation, average crystallite size, and lattice parameter. Fig. 1 shows the XRD patterns of all SiO_2 coated $Co_{1-x}Zn_xFe_2O_4$ nanoparticle samples with different values of Zn concentration

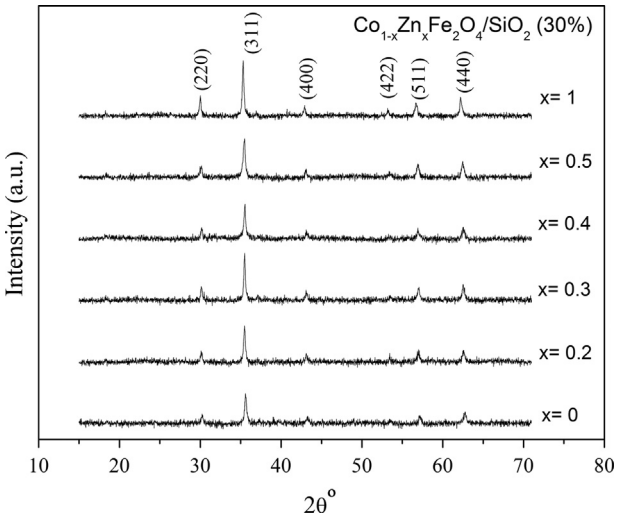

Fig. 1. XRD patterns of SiO_2 coated $Co_{1-x}Zn_xFe_2O_4$ nanoparticles with $x=0$, 0.2, 0.3, 0.4, 0.5 and 1.

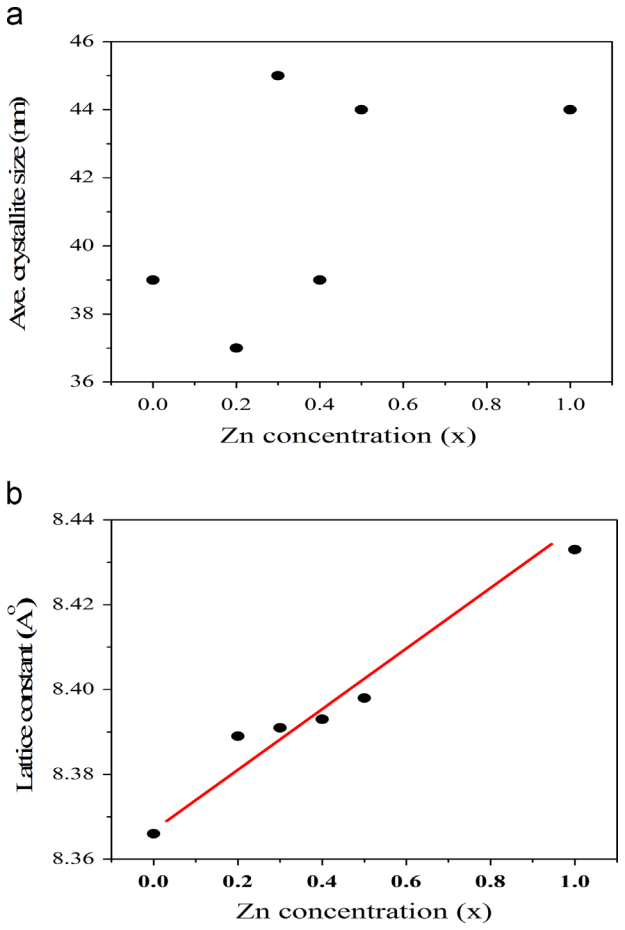

Fig. 2. (a) Average crystallite size of SiO_2 coated $Co_{1-x}Zn_xFe_2O_4$ nanoparticles as a function of Zn concentration (x)=0, 0.2, 0.3, 0.4, 0.5 and 1, and (b) lattice constant 'a' as a function of Zn concentration (x). Solid lines just show the trend.

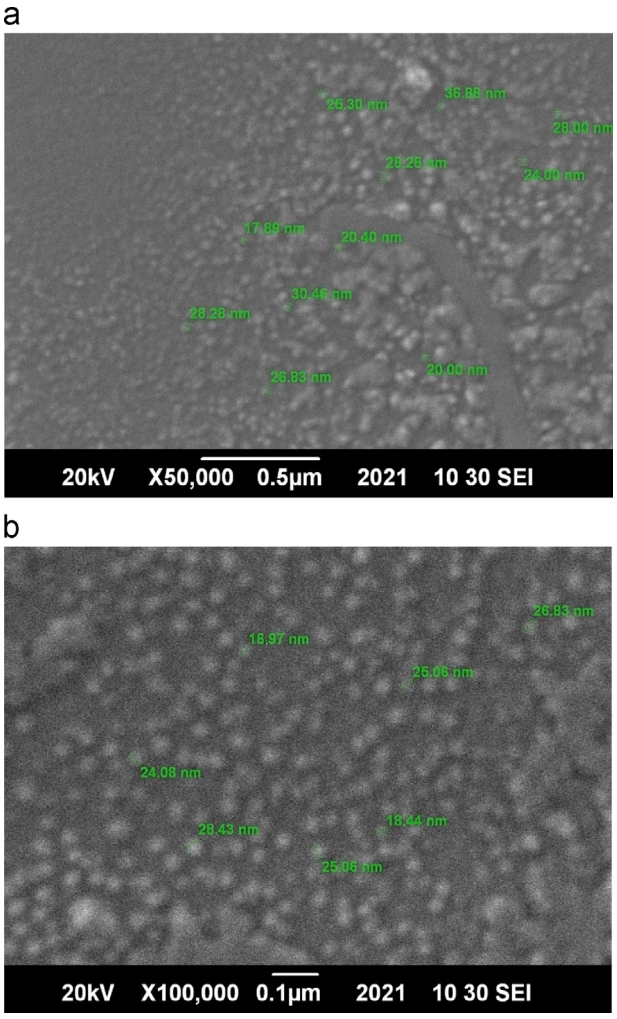

Fig. 3. SEM images of SiO_2 coated $CoFe_2O_4$ (x=0) nanoparticles at (a) scale=0.5 μm (500 nm), and (b) and scale=0.1 μm (100 nm).

(x)=0, 0.2, 0.3, 0.4, 0.5 and 1. It has been observed by using XRD reference cards JCPDS 22-1086 for $CoFe_2O_4$ and JCPDS 82-1092 for $ZnFe_2O_4$ that all the samples have spinel cubic ferrite structure without any other impurity phases. Average crystallite size is calculated by using Debye–Scherrer's formula. Fig. 2(a) shows the variation of average crystallite size with Zn concentration, which lies in the range 37–45 nm for different Zn concentrations. Although, we tried our best to kept the experimental conditions constant but still we got a non-monotonic behavior of average crystallite size with increasing Zn concentration, which may be due to inhomogeneous stirring, different gel formation time, etc. The variation of lattice constant 'a' as the function of Zn concentration is shown in Fig. 2(b). Lattice constant shows a monotonic increasing trend with increasing Zn concentration and is attributed to larger ionic radius of the Zn^{2+} ion (0.82 Å) as compared to Co^{2+} ion (0.78 Å) [25,35,36].

Scanning electron microscopy (SEM) was used to study the shape and size of the SiO_2 coated CoZn-ferrite nanoparticles. Fig. 3(a) and (b) shows the SEM images of one of the sample SiO_2 coated $CoFe_2O_4$ (x=0) nanoparticles at different scales. It has been observed that most of the nanoparticles are non-agglomerated due to the presence of non-magnetic SiO_2. SiO_2 surface coating act as a spacer between the nanoparticles and hence reduces agglomeration. The nanoparticles exhibit narrow particle size distribution and are nearly spherical in shape as evident from Fig. 3(b).

Fourier transform infrared (FTIR) spectroscopy is an important tool to explore the nature of local chemical bonds in a material. As XRD does not provide an evidence of amorphous SiO_2 surface coating (see Fig. 1), we used FTIR spectroscopy to unfold the features of SiO_2, ferrite, and also nanoparticle/SiO_2 interactions. Fig. 4(a) shows the FTIR absorption spectrum of KBr palletized SiO_2 coated $CoFe_2O_4$ (x=0) nanoparticles in the range 400–1200 cm^{-1}. The absorption bands at 453 and 565 cm^{-1} are due to the vibration of the chemical O–$M_{Oct.}$–O bond at octahedron position and chemical O–$M_{tet.}$–O bond at tetrahedron position of $CoFe_2O_4$ nanoparticle, respectively [37,38]. The presence of these absorption bands indicates the formation of spinel ferrite structure. The absorption bands at 800 and 1096 cm^{-1} correspond to symmetric and asymmetric stretching Si–O–Si vibrations, respectively, which confirm the formation of amorphous SiO_2 [39,40]. There are no signs of SiO_2–$CoFe_2O_4$

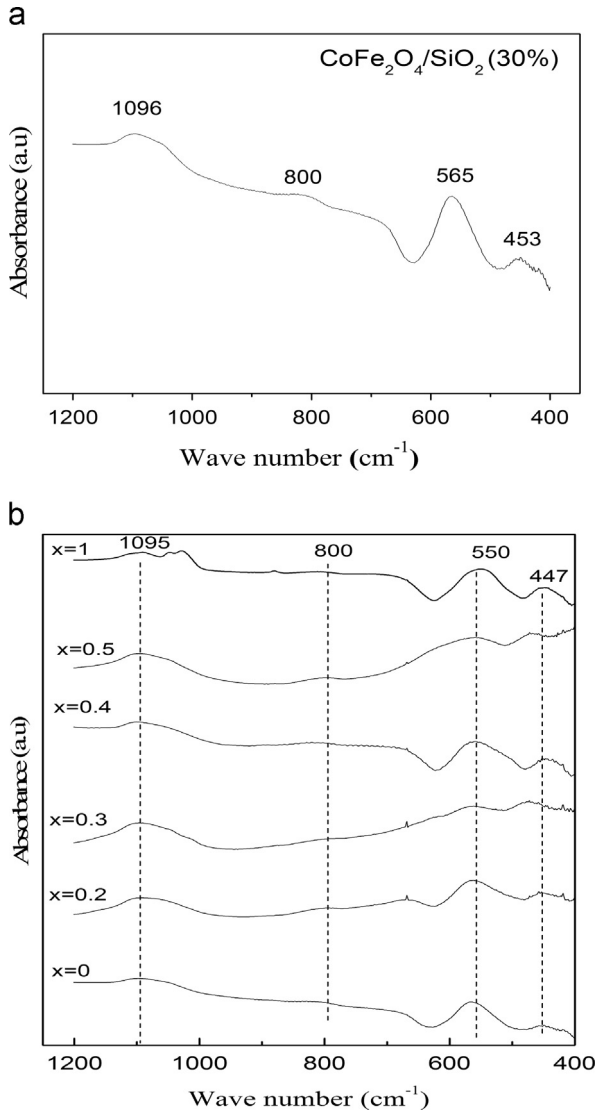

Fig. 4. (a) FTIR spectrum of SiO_2 coated $CoFe_2O_4$ ($x=0$) nanoparticles, and (b) FTIR spectra of all SiO_2 coated $Co_{1-x}Zn_xFe_2O_4$ nanoparticle samples with different Zn concentrations (x)=0, 0.2, 0.3, 0.4, 0.5 and 1. Dotted lines are drawn just for indication of the bands in different samples.

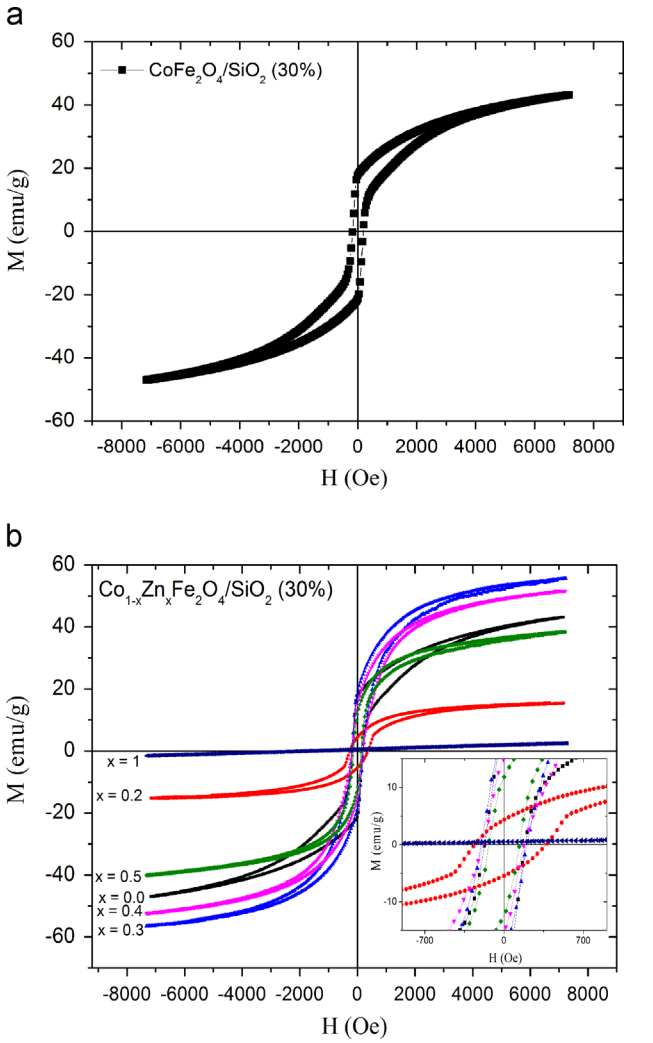

Fig. 5. (a) M–H loops of SiO_2 coated $CoFe_2O_4$ ($x=0$) nanoparticles, and (b) M–H loops of all SiO_2 coated $Co_{1-x}Zn_xFe_2O_4$ nanoparticle samples for different Zn concentrations (x)=0, 0.2, 0.3, 0.4, 0.5 and 1. Inset shows the coercivity region.

interaction band such as Fe–O–Si, which is usually found around 950 cm^{-1}. Fig. 4(b) shows the FTIR spectra of all the SiO_2 coated $Co_{1-x}Zn_xFe_2O_4$ ($x=0$, 0.2, 0.3, 0.4, 0.5, and 1) nanoparticle samples. The FTIR spectra provide evidence about the formation of ferrite and SiO_2 in all the samples.

Magnetization measurements were performed using a vibrating sample magnetometer (VSM) at room temperature with a maximum applied magnetic field of ± 7 kOe. Fig. 5(a) shows the M–H loops of SiO_2 coated $CoFe_2O_4$ ($x=0$) nanoparticles. The magnetic moments are not saturated due to low applied magnetic fields (± 7 kOe). The maximum magnetization for $CoFe_2O_4$ nanoparticles is 45.1 emu/g (after subtracting SiO_2 weight contribution), which is less than the saturation magnetization of bulk $CoFe_2O_4$ (74.08 emu/g) [41]. In ferrite nanoparticles, surface anisotropy is usually different from the bulk anisotropy due to disordered surface spins. The disordered surface spins are responsible for the lower magnetization in ferrite nanoparticles as compared to their counter bulk material [42]. The surface atoms have coordination bonds with the inner atoms only, which make dangling bonds on the individual nanoparticle's surface [43]. It is also observed that the magnetization of the SiO_2 coated $CoFe_2O_4$ nanoparticles is less than the bare $CoFe_2O_4$ nanoparticles of the same average particle size. This decrease in magnetization for the coated nanoparticles may be due to lesser agglomeration because agglomerated bare nanoparticles can give a combined magnetic effect. The M–H loops of all SiO_2 coated $Co_{1-x}Zn_xFe_2O_4$ nanoparticle samples with different Zn concentrations (x)=0, 0.2, 0.3, 0.4, 0.5, and 1 are shown in Fig. 5(b). Pure $CoFe_2O_4$ ($x=0$) nanoparticles show a ferrimagnetic behavior due to their inverse spinel structure in which Co^{2+} cations prefer the octahedral sites. On the other hand, pure $ZnFe_2O_4$ ($x=1$) nanoparticles show paramagnetic behavior due to its normal spinel structure in which Zn^{2+} ions prefer tetrahedral sites. The ferrimagnetic behavior of the nanoparticles decreases

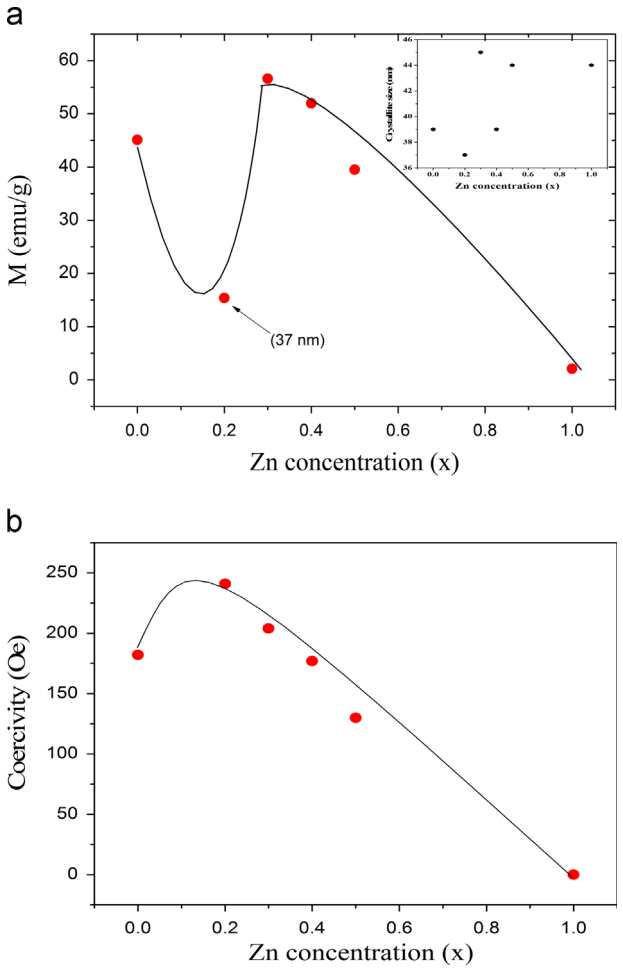

Fig. 6. (a) Variation of magnetization of SiO_2 coated $Co_{1-x}Zn_xFe_2O_4$ nanoparticles as a function of Zn concentration (x). Inset shows the variation of crystallite size with Zn concentration (x), and (b) variation of coercivity of SiO_2 coated $Co_{1-x}Zn_xFe_2O_4$ nanoparticles as a function of Zn concentration (x). Solid lines in both figures just show the trends.

with increasing Zn concentration (x) and finally we get paramagnetic behavior for $x=1$ sample (pure $ZnFe_2O_4$).

Fig. 6(a) and (b) shows the magnetization at 7 kOe ($M_{7\,kOe}$) and coercivity (H_c) of SiO_2 coated $Co_{1-x}Zn_xFe_2O_4$ nanoparticles as a function of Zn concentration (x). The magnetization shows a maximum at $x=0.3$ and then it decreases down to $x=1$. There are different reports about this particular Zn concentration to get maximum magnetization in $Co_{1-x}Zn_xFe_2O_4$ ferrite [17,23–25]. The Zn^{2+} ions prefer tetrahedral lattice sites in the normal spinel structure of $ZnFe_2O_4$. The existence of magnetization peak reveals that the Zn^{2+} ions prefer different lattice sites before and after the peak position, otherwise we should get a monotonic behavior. The decrease in the magnetization at higher Zn concentration ($x>0.3$) is due to the reduction of exchange interaction between tetrahedral (A) and octahedral (B) lattice sites ions, which finally results in the weakening of A–B interactions and leads to the destabilization of the magnetic ordering. It is difficult to prepare nanoparticles with nearly same size using chemical methods due to a lot of experimental parameters, which can affect the nanoparticle diameter. The decrease of magnetization with the decreasing ferrite nanoparticle's diameter is a well-known effect due to significant importance of surface to volume ratio in the nanoparticles. The atoms on the surface have less coordination neighbors due to which their mutual exchange interactions are reduced. Therefore the effect of nanoparticle crystallite size on magnetization should also be considered while studying the doping effects. In our case, average crystallite size varies non-monotonically with the increase of Zn concentration (x). For convenience, we have shown the variation of the average crystallite size with Zn concentration (x) in the inset of Fig. 6(a). The magnetization dip for nanoparticles with $x=0.2$ Zn concentration is due to their smaller average crystallite size (37 nm). The average crystallite size affects the nanoparticle magnetization more dominantly in the regime $x=0-0.3$ due to less Zn concentration (x). However above $x>0.3$, Zn concentration dominates in determining the magnetization e.g., magnetization of nanoparticles with $x=0.5$ and 1 is lower than $x=0.3$, although their average crystallite size is comparable. Therefore both average crystallite size and Zn doping compete each other in this system. For $x>0.2$, the H_c decreases with increasing Zn concentration (x) and is attributed to smaller anisotropy of Zn^{2+} ions as compared to Co^{2+} ions. In the literature, it is reported that the H_c also depends on the nanoparticle size. The surface anisotropy increases with decreasing particle size due to more disordered surface spins and can give larger coercivity. Nanoparticles with $x=0.2$ exhibit maximum H_c due to their smaller average crystallite size of 37 nm. Pure $ZnFe_2O_4$ ($x=1$) nanoparticles show nearly zero H_c due to their paramagnetic nature.

4. Conclusions

SiO_2 coated $Co_{1-x}Zn_xFe_2O_4$ nanoparticles (with $x=0$, 0.2, 0.3, 0.4, 0.5, and 1) were successfully prepared by using the sol–gel method. XRD, SEM and FTIR were used for the structural and morphological studies. XRD study revealed cubic spinel ferrite structure for all the samples. The average crystallite size lies in the range of 37–45 nm. The lattice constant showed an increasing trend with increasing Zn concentration and is attributed to the larger ionic radii of Zn^{2+} ions as compared to Co^{2+} ions. FTIR spectroscopy confirmed the formation of ferrite and SiO_2. SEM images showed that the nanoparticles are spherical in shape, narrow particle size distribution and non-agglomerated due to presence of non-magnetic SiO_2 surface coating. The magnetization exhibits a maximum at $x=0.3$, after which it shows a decreasing trend due to change in cationic distribution. The changes in magnetic behavior are attributed to the redistribution of cations between octahedral (B) and tetrahedral (A) lattice sites upon doping Zn^{2+} ions. The coercivity first increases from $x=0$ to $x=0.2$ and then decreases down to $x=1$. The decrease in coercivity for $x>0.2$ is due to smaller anisotropy of Zn^{2+} ions as compared to Co^{2+} ions. It can be concluded that the structural and magnetic properties of SiO_2 coated $Co_{1-x}Zn_xFe_2O_4$ ferrite nanoparticles strongly depend

upon the concentration of Zn^{2+} ions and average crystallite size in different regimes of Zn doping.

Acknowledgment

Higher Education Commission of Pakistan is acknowledged for providing research funds.

References

[1] G. Cao, in: Nanostructures and Nanomaterials Synthesis, Properties and Applications, Imperial College Press, London, 2003.
[2] J. Smit, H.P.J. Wijn, in: Ferrites: Physical Properties of Ferromagnetic Oxides in Relation to their Technical Applications, Wiley, New York, 1959.
[3] R.C.O' Handely, in: Modern Magnetic Materials Principles and Applications, John Wiley and Sons, New York, 2000.
[4] Dino Fiorani, in: Surface Effects in Magnetic Nanoparticles, 1st ed., Springer, New York, 2005.
[5] D. Fiorani, A.M. Testa, F. Lucari, F. D'Orazio, H. Romero, Physica B 320 (2002) 122–126.
[6] R.H. Kodama, J. Magn. Magn. Mater. 200 (1999) 359–372.
[7] R.H. Kodama, A.E. Berkowitz, E.J. Mcniff, S. Foner, Phys. Rev. Lett. 77 (1996) 394–397.
[8] K. Nadeem, H. Krenn, T. Traussing, I. Letofsky-Papst, J. Appl. Phys. 109 (2011) 013912.
[9] K. Nadeem, H. Krenn, T. Traussnig, R. Würschum, D.V. Szabó, I. Letofsky-Papst, J. Appl. Phys. 111 (2012) 113911.
[10] A. Goldman, in: Modern Ferrite Technology, Van Nostard Reinhold, New York, 1990.
[11] Lijun Zhao, Hua Yang, Xueping Zhao, Lianxiang Yu, Yuming Cui, Shouhua Feng, Mater. Lett. 60 (2006) 1–6.
[12] L. Ben Tahar, M. Artus, S. Ammar, L.S. Smiri, F. Herbst, M.-J. Vaulay, V. Richard, J.-M. Grenèche, F. Villain, F. Fiévet, J. Magn. Magn. Mater. 320 (2008) 3242–3250.
[13] J.A. Paulsen, A.P. Ring, C.C.H. Lo, J.E. Snyder, D.C. Jiles, J. Appl. Phys. 97 (2005) 044502.
[14] Myrtil L. Kahn, Z. John Zhang, Appl. Phys. Lett. 78 (2001) 3651.
[15] S.D. Bhame, P.A. Joy, J. Phys. D 40 (2007) 3263.
[16] Jianhong Peng, Mirabbos Hojamberdiev, Yunhua Xu, Baowei Cao, Juan Wang, Hong Wu, J. Magn. Magn. Mater. 323 (2011) 133–137.
[17] S. Singhal, T. Namgyal, S. Bansal, K. Chandra, J. Electromagn. Anal. Appl. 2 (2010) 376–381.
[18] G. Vaidyanathan, S. Sendhilnathan, R. Arulmurgan, J. Magn. Magn. Mater. 313 (2007) 293–299.
[19] W. Bayoumi, J. Mater. Sci. 42 (2007) 8254–8261.
[20] G.A. Sawatzky, F. Woude, A.H. Morrish, J. Appl. Phys. 39 (1968) 1204.
[21] G.A. Sawatzky, F. Woude, A.H. Morrish, Phys. Rev. 187 (1969) 747–757.
[22] M.R. De Guire, R.C.O' Handley, G. Kalonji, J. Appl. Phys. 65 (1989) 3167–3172.
[23] Chengyi Hou, Hao Yu, Qinghong Zhang, Yaogang Li, Hongzhi Wang, J. Alloys Compd. 491 (2010) 431–435.
[24] N. Somaiah, T.V. Jayaraman, P.A. Joy, D. Das, J. Magn. Magn. Mater. 324 (2012) 2286–2291.
[25] R. Rani, S.K. Sharma, K.R. Pirota, M. Knobel, S. Thakur, M. Singh, Ceram. Int. 38 (2012) 2389–2394.
[26] G. Li, S. Yan, E. Zhou, Y. Chen, Colloids Surf. A 276 (2006) 40–44.
[27] K.H. Wu, Y.C. Chang, T.C. Chang, Y.S. Chiu, T.R. Wu, J. Magn. Magn. Mater. 283 (2004) 380–384.
[28] S. Zhang, D. Dong, Y. Sui, Z. Liu, H. Wang, Z. Qian, W. Su, J. Alloys Compd. 415 (2006) 257–260.
[29] J.B. da Silva, N.D.S. Mohallem, J. Magn. Magn. Mater. 226–230 (2001) 1393–1396.
[30] K. Nadeem, T. Traussning, I. Letofsky-Papst, H. Krenn, U. Brossmann, R. Wörschum, J. Alloys Compd. 493 (2010) 385–390.
[31] Shik Chi Tsang, Chih Hao Yu, Xin Gao, Kin Tam, J. Phys. Chem. B 110 (2006) 16914–16922.
[32] Hongxia Wang, Wei Zhang, Faling Zhang, Yuan Cao, Wenhui Su, J. Magn. Magn. Mater. 320 (2008) 1916–1920.
[33] K.H. Wu, Y.C. Chang, G.P. Wang, J. Magn. Magn. Mater. 269 (2004) 150–155.
[34] Yong-Hui Deng, Chang-Chun Wang, Jian-Hua Hu, Wu-Li Yang, Shou-Kuan Fu, Colloids Surf. A 262 (2005) 87–93.
[35] R. Arulmurugam, B. Jeyadevan, G. Vaidyanathan, S. Sendhilnathan, J. Magn. Magn. Mater. 288 (2005) 470–477.
[36] I.H. Gul, A.Z. Abbasi, F. Amin, M. Anis-ur-Rehman, A. Maqsood, J. Magn. Magn. Mater. 311 (2007) 494–499.
[37] A. Pradeep, P. Priyadharsini, G. Chandrasekaran, Mater. Chem. Phys. 112 (2008) 572–576.
[38] M.K. Shobana, V. Rajendran, K. Jeyasubramanian, N.S. Kumar, Mater. Lett. 61 (2007) 2616–2619.
[39] K.H. Wu, W.C. Huang, J. Solid State Chem. 177 (2004) 3052–3057.
[40] S.N. Dang, S.X. Lu, W.G. Xu, J. Sa, J. Non-Cryst. Solids 354 (2008) 5018–5021.
[41] M.P. Gonzalez-Sandoval, A.M. Beesley, M. Miki-Yoshida, L. Fuentes-Cobas, J.A. Matutes-Aquino, J. Alloys Compd. 369 (2004) 190–194.
[42] R.H. Kodama, A.E. Berkowitz, E.J. McNiff, S. Foner, J. Appl. Phys. 81 (1997) 5552–5557.
[43] X. Batlle, A. Labarta, J. Phys. D 35 (2002) R15.